Adsorption (2015) 21:307–320
DOI 10.1007/s10450-015-9672-x

Saturation loadings on 13X (faujasite) zeolite above and below the critical conditions. Part I: alkane data evaluation and modeling

Alaa Al Mousa[1] · **Dana Abouelnasr**[2,3] · **Kevin F. Loughlin**[2]

Received: 5 March 2014 / Revised: 3 April 2015 / Accepted: 9 April 2015 / Published online: 22 April 2015

Abstract The saturation loadings for subcritical adsorption of n-, iso- and neo alkanes C_1–C_8 in 13X zeolite are modeled using the modified Rackett model of Spencer and Danner (J Chem Eng Data 17:236–240, 1972) for the saturated liquid densities combined with crystallographic data for the 13X zeolite. For validation of this model, alkane adsorption data in the literature is first critically evaluated and then compared to the model. The saturation loading of each isotherm that approaches saturation is extracted from the data. Log–log plots are used to determine whether each isotherm is near saturation; isotherms that exhibit a $(\partial \ln q)/(\partial \ln p)$ slope of zero at their maximum pressure point are assumed to be saturated. Isotherms not fulfilling this criterion are deemed unsaturated and not considered further. The theoretical equation satisfactorily models the available experimental data for the n- alkanes. However, steric factors are required for the model to fit iso alkanes and neo-pentane. For supercritical temperatures, no model presently exists to explain the data. However, the data are satisfactorily modeled with an equation of the form $q_{max} = 8.5 \pm 2.5$ g/100 g.

Keywords Alkanes C_1–C_8 · 13X zeolite · Sorbate densities · Saturation loadings · Sorbate molar volumes · Critical conditions

List of symbols

Variables

MW	Molecular weight (g/mol)
P_c	Critical pressure (kPa)
P_r	Reduced pressure
q	Zeolite loading (g/100 g zeolite crystal)
q_{max}	Maximum zeolite loading (g/100 g zeolite crystal)
$q_{max,c}$	Theoretical maximum zeolite loading at the critical temperature, defined by Eq. 5 (g/100 g zeolite crystal)
R	Gas constant (8314 kPa-cm^3/gmol.K)
T_c	Critical temperature (K)
T_{CAR}	Critical adsorbate reduced temperature (K)
T_r	Reduced temperature
V_{sat}	Saturated liquid volume (cm^3/g)
Z_{RA}	Rackett parameter

Greek letters

Γ	Normalized loading, dimensionless, calculated in Eqs. 6 and 7
ε_Z	Crystallographic 13X zeolite void fraction, 0.428 (Breck 1974, p. 133)
λ	Steric factor, used in Eq. 8
ρ_{sat}	Sorbate liquid density, g adsorbate/cm$^{3)}$
ρ_Z	Zeolite 13X crystallographic density, 1.43 g/cm^3, (Breck 1974, p. 133)

Kevin F. Loughlin—American University of Sharjah (retired).

Electronic supplementary material The online version of this article (doi:10.1007/s10450-015-9672-x) contains supplementary material, which is available to authorized users.

✉ Dana Abouelnasr
dabouelnasr@aus.edu

Kevin F. Loughlin
kff.loughlin@gmail.com

[1] Petrofac International Ltd, Sharjah, UAE

[2] Department of Chemical Engineering, American University of Sharjah, P.O. Box 26666, Sharjah, UAE

[3] California State University at Bakersfield, Bakersfield, USA

1 Introduction

In the prediction of model isotherms for adsorbents, modeling parameters are always required. One of the most frequently required is the saturation loading. In this manuscript, a simple concept for sorbate density is proposed to establish the saturation loadings of subcritical alkanes on 13X zeolite. The authors collected data from the literature for the adsorption of straight-chain and branched hydrocarbons on 13X zeolite and analyzed this data thoroughly for consistency between studies and for saturation conditions. The focus is on acquiring as much adsorption data near saturation as possible. Then the maximum adsorbed amount for each isotherm at or near saturation is compared to a model for q_{max} which uses crystallographic data for 13X and the modified Rackett model for the specific volume of saturated liquids to estimate the sorbate density.

2 Theoretical model

The following model was previously presented in the paper of (Loughlin and Abouelnasr 2009). A brief synopsis is given here. The theoretical saturation loading of several alkanes in 13X zeolite may be calculated from first principles for zeolite crystals assuming 100 % accessibility for the alkanes, as:

$$q_{\max}\left(\frac{g}{100gZ}\right) = 100\frac{\varepsilon_Z \rho_{sat}}{\rho_Z}, \tag{1}$$

where ε_Z is the zeolite void fraction, ρ_{sat} is the sorbate liquid density, and ρ_Z is the zeolite crystallographic density. In this equation the saturation density for liquids below the critical point is calculated using the modified Rackett equation:

$$V_{sat} = \frac{1}{\rho_{sat}} = \left(\frac{RT_c}{P_c\mathrm{MW}}\right) Z_{RA}^{\left\{1+(1-T_r)^{0.2857}\right\}}. \tag{2}$$

Z_{RA} is a particular constant for the modified Rackett equation; values are given in the paper by Spencer and Danner 1972. In addition, values for all the critical constants and the Rackett parameter Z_{RA} are also given on the (CHERIC 2012) website. The modified Rackett equation is reported to be a ± 2.4 % improvement over the Rackett equation Spencer and Danner 1972.

Combining Eqs. 1 and 2 gives the final equation for q_{max}.

$$q_{\max}\left(\frac{g}{100gZ}\right) = 100\frac{\varepsilon_Z}{\rho_Z}\left(\frac{P_c\mathrm{MW}}{RT_c}\right) Z_{RA}^{-\left\{1+(1-T_r)^{0.2857}\right\}}. \tag{3}$$

An alternative expression is:

$$q_{\max}\left(\frac{g}{100gZ}\right) = q_{\max,c} Z_{RA}^{-(1-T_r)^{0.2857}}, \tag{4}$$

where $q_{max,c}$ is the theoretical loading at critical conditions:

$$q_{\max,c} = 100\frac{\varepsilon_Z}{\rho_Z}\left(\frac{P_c\mathrm{MW}}{RT_c Z_{RA}}\right). \tag{5}$$

However, we previously observed that the critical reduced temperature for adsorbed alkanes, T_{CAR}, can differ from the vapor–liquid critical temperature (Loughlin and Abouelnasr 2009). T_{CAR} for methane, ethane, and larger n alkanes was found to occur at a T_r of 0.83, 0.96, and 0.975, respectively, for 5A zeolite.

A theoretical plot of q_{max} versus reduced temperature calculated using Eq. 3 is presented in Fig. 1 and in Figure S1 in the supplementary information for all the n alkanes ranging from C_1 to C_8 used in this study. The maximum loading decreases monotonically with reduced temperature and rapidly decreases as $T_r = 1$ is approached. This is a reflection of the increased rotational and vibrational energy of the molecules as the temperature increases. At any particular T_r, the saturation loading increases from C_1 to C_8. The models for the iso alkanes and for the neo alkane are very similar in both shape and position.

Equation 4 may be rearranged to give a normalized value for the loading Γ by taking logarithms.

$$\Gamma = (1 - T_r)^{0.2857}, \tag{6}$$

where Γ is given by Eq. 7.

$$\Gamma = -\frac{\ln\left(q_{\max}/q_{\max,c}\right)}{\ln(Z_{RA})}. \tag{7}$$

Using Γ, the experimentally observed values for q_{max} may be plotted for all substances using Eq. 7 on a single graph, and compared to the theoretical curve, given by Eq. 6.

3 Methodology

In performing a study like this, the quality of the 13X molecular sieves or faujasite zeolites should be the same. However, the formula of the zeolites used in these studies is seldom reported. We have assumed a hydrated formula weight similar to the 13X zeolite reported in the text by Breck (1974)–$Na_{86}[(AlO_2)_{86}(SiO_2)_{106}]264H_2O$. This is the formula weight used in the Linde 13X molecular sieve. Various forms of X and Y zeolite exist. Where differences exist such as in the zeolites used in the studies of Campo et al (2013, 2014), these studies have been considered, but ultimately not used because they differ from other relevant studies. The simple reason is that the pore size varies for

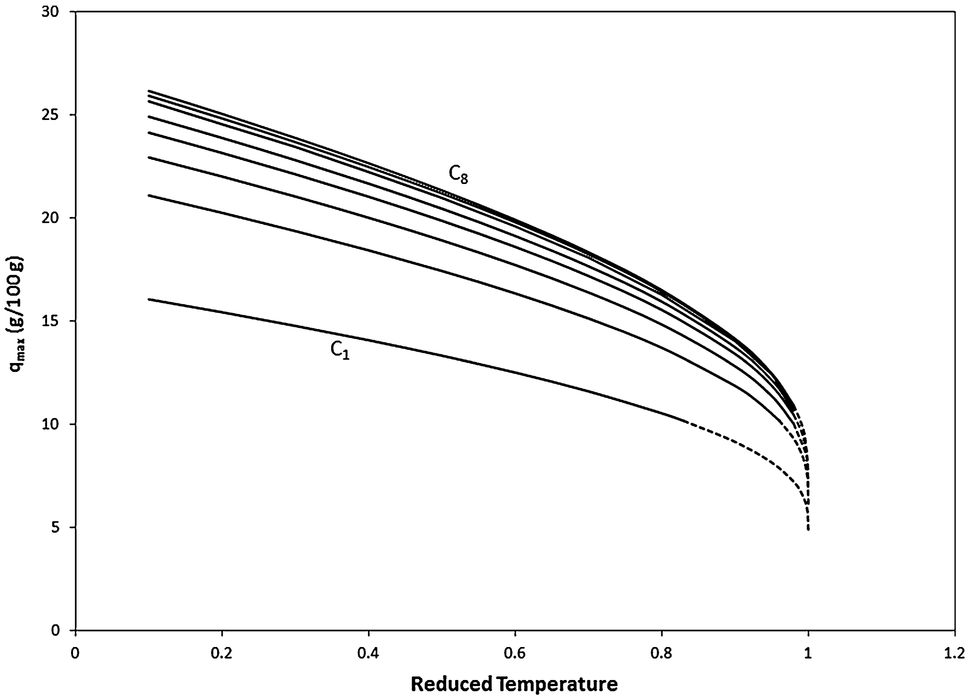

Fig. 1 q_{max} calculated from Rackett's equation and crystal properties for n-alkanes C_1 through C_8 as a function of reduced temperature. A *dashed line* is used when T_r is above the T_{CAR} for 5A zeolite (Loughlin and Abouelnasr 2009) for the given species

different forms of X or Y zeolite, and when the authors clearly state a different 13X zeolite, the isotherms are not comparable to isotherms from other studies, and the studies are excluded. The assumption of similar formula weight used by Breck is a limitation of this study.

Experimental data for isotherms of straight-chain and branched alkanes on 13X are collected from the literature. Other substances (cyclic alkanes, alkenes, aromatics and inorganics) are also considered and are reported (Al Mousa et al. 2015a, b) separately. Untabulated adsorption data on NaX, faujasite or Linde, CECA or other 13X zeolite (labelled 13X hereafter) are reported by digitizing the appropriate figures. The data has been systematically evaluated for consistency using the same criteria as reported in the paper of Loughlin and Abouelnasr 2009.

The adsorption isotherms extracted from the literature are summarized in Table 1 for subcritical and supercritical data. In column 1 is the authors' names and the date of the study. In column 2, species and the reduced temperatures of the adsorption isotherms are specified. In column 3 are comments, including the adsorbent, the percentage binder, and the reason why a particular study might not be used. For example, (Lopes et al. 2009) did not mention the % binder, and so is omitted from further consideration. In this case, the supplier of the zeolite they used in the study was contacted, but this proved fruitless.

The isotherms in Table 1 are plotted by species for the purpose of determining their consistency as per the criteria mentioned above. The isotherms are first examined on a q versus ln P_r plot. Inconsistent isotherms or inconsistent data points are removed. The reasons for their removal are stated for each figure. The isotherms are then plotted on a ln q versus ln P_r plot. For methane an intermediate plot of q versus ln P_r is also included to illustrate the effects of the deletions. Isotherms passing the data consistency criteria are then assessed according to the criteria for choosing the saturation loading from experimental data. Only isotherms which are saturated or are approaching saturation are considered further as determined when the slope of the ln q versus ln P_r plot approaches zero. Isotherms far from saturation are not included in the q_{max} observations. In addition to assessing the isotherms to determine whether they attain saturation, we also comment on their consistency with Henry's law at low loadings $\left(\frac{d\ln q}{d\ln p} = 1\right)$ where appropriate.

4 Results and discussion

We begin with an assessment of the data quality for each substance. All the isotherms are plotted in supplementary data denoted by symbol S. Critical isotherms are retained in the manuscript.

The methane isotherms before screening are plotted in Figs. 2a and S2a. They range from a T_r of 0.47 to 1.84. Isotherms from 6 different studies are included. The shape of some of the isotherms appears inconsistent. The Cavenati et al. (2004) isotherms are deleted completely as they suffer from inconsistency in position and shape crossing

Table 1 Studies reporting straight-chain and branched alkane adsorption onto 13X zeolite

Source	Isotherm reduced temperature	Comment
Barrer and Sutherland (1956)	C_1: 0.47, 1.02, 1.43, 1.56	Isotherms plotted on a hydrated basis have been corrected to a dehydrated basis per the % hydration indicated in the paper
	C_2: 0.64, 0.90, 0.98, 1.00	
	C_3: 0.53, 0.83, 0.87	
	nC_4: 0.70, 0.71, 0.72, 0.74, 0.75, 0.76, 0.77, 0.78, 0.80, 0.81	
	iC_4: 0.73, 0.74, 0.76, 0.77, 0.78, 0.79, 0.80, 0.82, 0.83, 0.84	
	nC_5: 0.63, 0.64, 0.66, 0.67, 0.68, 0.69, 0.70, 0.71, 0.72, 0.73	
	iC_5: 0.65, 0.66, 0.67, 0.68, 0.69, 0.70, 0.71, 0.72, 0.73, 0.74	
	neo-C_5: 0.69, 0.70, 0.71, 0.72, 0.73, 0.74, 0.76, 0.77, 0.78, 0.79	
	nC_6: 0.59, 0.60, 0.61, 0.62, 0.63, 0.64, 0.65, 0.66, 0.67, 0.68	
	nC_7: 0.55, 0.56, 0.57, 0.58, 0.59, 0.60, 0.61, 0.62, 0.63, 0.64	
	iC_8: 0.55, 0.56, 0.57, 0.58, 0.585, 0.59, 0.60, 0.61, 0.62, 0.63	
	nC_8: 0.55, 0.57, 0.59, 0.60	
Campo et al. (2013)	C_3: 0.87, 1.01, 1.14	CECA France beads, 11 % binder
Campo et al. (2014)	iC_4: 0.79, 0.92, 1.04	CECA France beads, 11 % binder
Cavenati et al. (2004)	C_1: 1.56, 1.62, 1.69	CECA France pellets, 17 % binder Deleted because they are inconsistent with other C_1 isotherms
Da Silva and Rodrigues (1999)	C_3: 0.82, 0.87, 0.93, 1.01, 1.14, 1.28	CECA France pellets, 17 % binder
Hyun and Danner(1982)	C_2: 0.90, 0.98, 1.06, 1.22	Union carbide pellets, 20 % binder
	iC_4: 0.73, 0.79, 0.92	
Lamia et al. (2007)	C_3: 0.90, 0.95, 1.01, 1.06	CECA France pellets, 17 % binder
	iC_4: 0.82, 0.87, 0.92, 0.96	
Lopes et al. (2009)	C_1: 1.59, 1.62, 1.69	Pellets of unknown percentage binder-deleted
Loughlin et al. (1990)	C_1: 1.44, 1.57, 1.71, 1.84	Union carbide pellets, 20 % binder
	C_3: 0.74, 0.81, 0.88, 0.95	
Narin et al. (2014)	C_2: 1.06, 1.22, 1.39	Chemiewerk bad köstritz GmbH binderless beads, 0 % binder
	C_3: 0.87, 1.01, 1.14	
Rolniak and Kobayashi (1980)	C_1: 1.51, 1.56, 1.62	Molecular sieve pellets, 20 % binder
Ruthven and Doetsch (1976)	nC_7: 0.76, 0.81, 0.85, 0.90	Union carbide crystal
Salem et al. (1998)	C_1: 1.35, 1.43, 1.51, 1.62, 1.67	Molecular sieve pellets, 20 % binder
van Miltenburg et al. (2008)	C_3: 0.86, 0.97, 1.09	Crystals
Vermesse et al. (1996)	C_1: 1.56	CECA France pellets, 17 % binder Excess isotherms
Zhdanov et al. (1962)	nC_6: 0.59	Union carbide pellets, 20 % binder

the rest of the isotherms. The methane isotherm from Vermesse et al. (1996) study is measured at pressures up to 500 MPa. This paper is unique in its pressure range for a laboratory scale study. Hence, its consistency at such high pressure could not be assessed and accordingly it is deleted. The methane isotherm from Barrer and Sutherland (1956) at a T_r of 0.47, or 90 K is unique as well. Its accuracy could also not be assessed but it is retained. Two of the isotherms are modified. The Barrer and Sutherland isotherm at T_r of 0.47 exhibits capillary condensation at the top end. These convex points are deleted (shown as grey points in the figure). The Barrer and Sutherland isotherm for C_1 at T_r of 1.02 is in agreement with the rest of the data in the low pressure region but the top points in the high pressure region are flattening and appear to approach crossing other isotherms in this region. These points are deleted (grey points in the figure). All the isotherms from Barrer and Sutherland (1956), Loughlin et al. (1990), Rolniak and Kobayashi (1980), and Salem et al. (1998) are retained. Figures 2b and S2b shows the methane isotherms after removing deleted isotherms and data points. The shapes of the isotherms are consistent in shape and position.

The isotherms of methane are also plotted on a log–log plot in Figs. 2c and S2c. As per the criteria for choosing the saturation loading from the experimental data, it may be observed that all methane isotherms are saturated since they

Fig. 2 **a** Methane isotherms before screening. Labels are reduced temperatures. Isotherms in *grey* are inconsistent with others, and so are screened out. Deleted points are in *grey*. **b** Methane isotherms after screening. Labels are reduced temperatures. Isotherms that attain saturation have a *solid line*. Isotherms that are not near saturation have a *dotted line*. **c** Log–log plot of methane isotherms. Labels are reduced temperatures. Isotherms that attain saturation have a *solid line*. Isotherms that are not near saturation have a *dotted line*

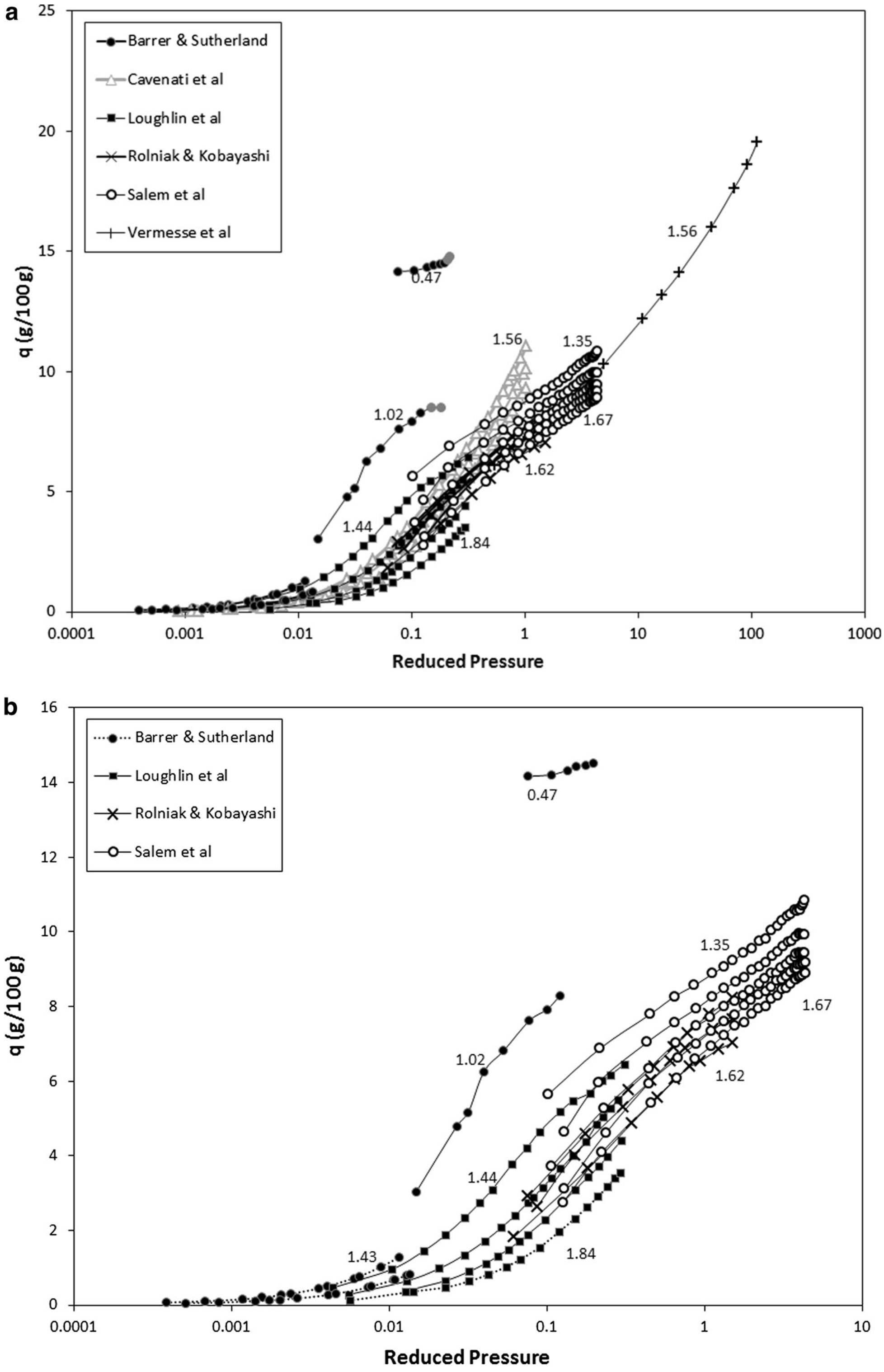

are leveling off with the exception of three only. These three isotherms, one from Loughlin et al. (1990) at a T_r of 1.84, and two from Barrer and Sutherland (1956) at a T_r of 1.43 and 1.56 are far from saturation and hence excluded from the saturation calculations. This is very clear when data are plotted as loading versus reduced pressure on a logarithmic scale. It should be noted that all the isotherms that extend into low loadings appear to have a $(\partial \ln q)/(\partial \ln p)$ slope of 1 consistent with Henry's law. There appears to be a slight kink in the T_r of 1.84 isotherm at the second lowest point.

Fig. 2 continued

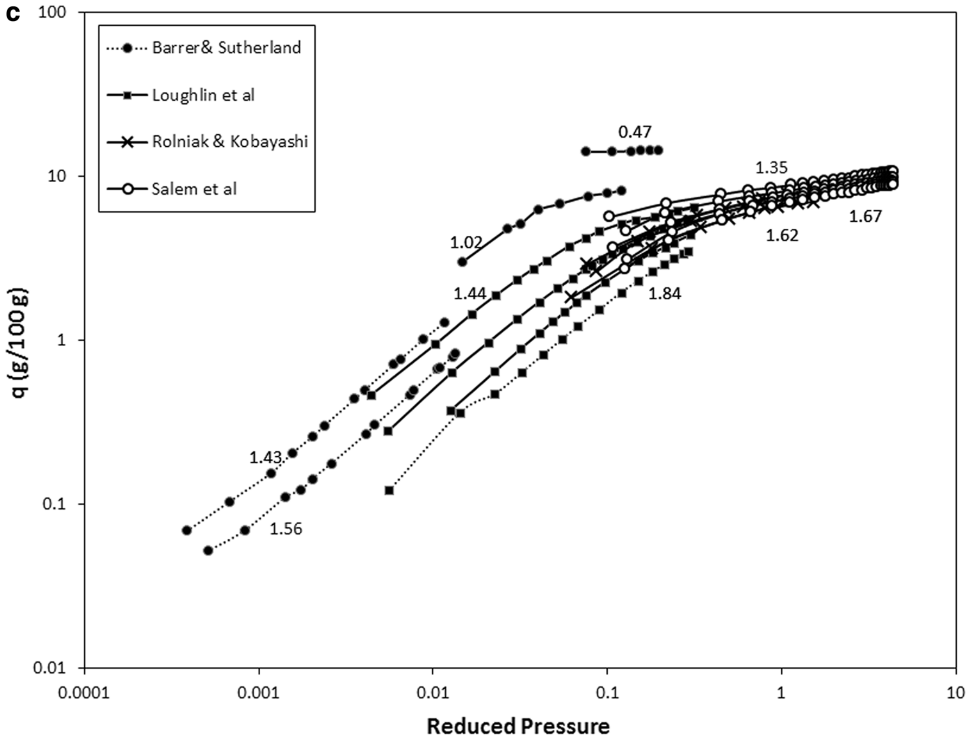

Adsorption isotherms for ethane without any modification are plotted in Figure S3a. The original data are extracted from the respective papers summarized in Table 1. Data from three different studies, Barrer and Sutherland (1956), Hyun and Danner (1982) and Narin et al. (2014) are included ranging from a T_r of 0.64 to 1.39. The isotherms appear to be consistent in shape but not in position. Isotherms from Barrer and Sutherland (1956) are higher than those for Hyun and Danner. However, both are adjacent to each other and it is difficult to ascertain which one of them is correct. Hence, both are retained. The isotherms of Narin et al. appear consistent with Hyun and Danner and are retained.

The isotherms are plotted on a log–log plot in Figs. 3 and S3b. As per the criteria for choosing the saturation loading from the experimental data, two isotherms, Hyun and Daner (1982) with a T_r of 1.22 and Narin et al. (2014) with a T_r of 1.39 are far from saturation and hence are excluded from the saturation observations. All other isotherms are leveling off and hence saturated. This is evident from ethane isotherms plotted on a logarithmic scale. It should be noted that all the isotherms that extend into low loadings appear to have a slope of 1 $\left(\frac{d\ln q}{d\ln p}=1\right)$ consistent with Henry's law, although there are slight kinks in four of the isotherms in this region.

Isotherms for propane before screening are plotted in Figure S4a. Temperatures range from a T_r of 0.53 to 1.28. Data are collected from seven different studies. These are for Barrer and Sutherland (1956), Campo et al. (2013), Da Silva and Rodrigues (1999), Lamia et al. (2007), van Miltenburg et al. (2008), Loughlin et al. (1990) and Narin et al. (2014). The shape of the Campo et al. (2013) isotherms appears to be inconsistent and so these isotherms are deleted. Also, two of the isotherms by Narin et al. [$T_r = 1.01$ and 1.14] appear out of position and are deleted. Five of the remaining isotherms are modified. The Barrer and Sutherland (1956) isotherm at T_r of 0.53 exhibits capillary condensation. The convex point is deleted (shown as a grey point in the figure). The lowest pressure point on four isotherms are out of place, and deleted (grey points). Isotherms from Barrer and Sutherland (1956) are slightly higher than the rest of the isotherms; however, they are close to the others and hence retained. The isotherms at $T_r = 0.86$ and 0.97 of van Miltenburg et al. (2008) are consistent with the other isotherms and are retained but the isotherm at $T_r = 1.09$ is inconsistent and is deleted (shown in grey).

The propane isotherms are plotted on a log–log scale in Figs. 4 and S4b. The solid lines which appear to be levelling out at high loadings are used to estimate the q_{max} values; the dotted lines do not meet this criteria and are not used for this purpose. At the low loadings, all the isotherms appear to have a slope of 1 in the Henry law region.

Adsorption isotherms for n butane are shown in Figures S5a and S5b. Straight chain butane data are found in a single study Barrer and Sutherland (1956). Figure S5a shows the straight butane isotherms ranging from a T_r of

Fig. 3 Log–log plot of ethane isotherms. Labels are reduced temperatures. Isotherms that attain saturation have a *solid line*. Isotherms that are not near saturation have a *dotted line*

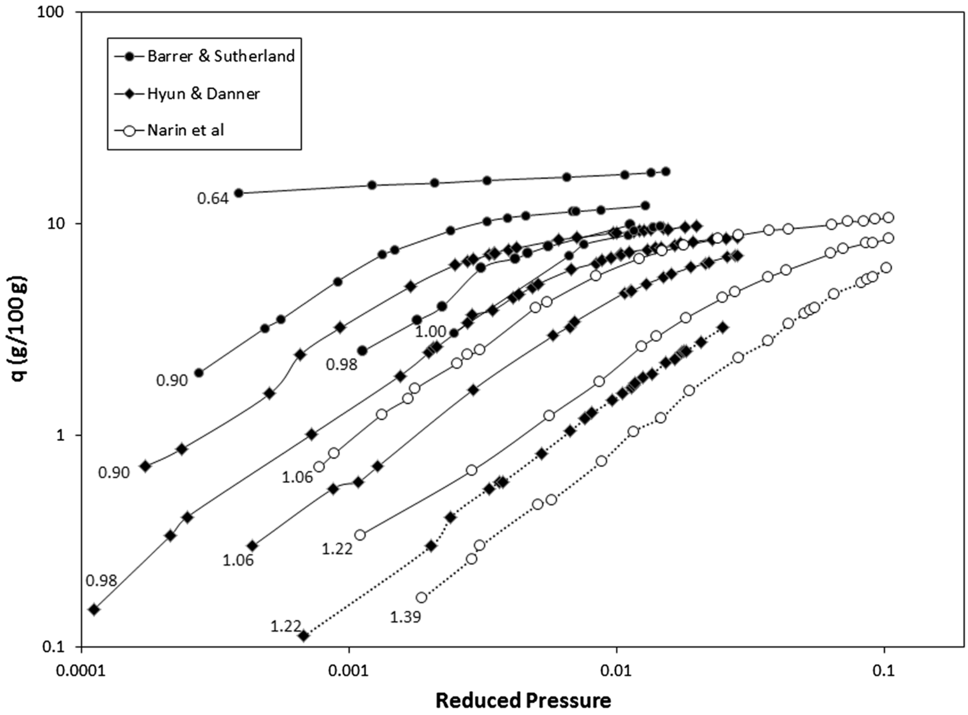

Fig. 4 Log–log plot of propane isotherms. Labels are reduced temperatures. Isotherms that attain saturation have a *solid line*. Isotherms that are not near saturation have a *dotted line*

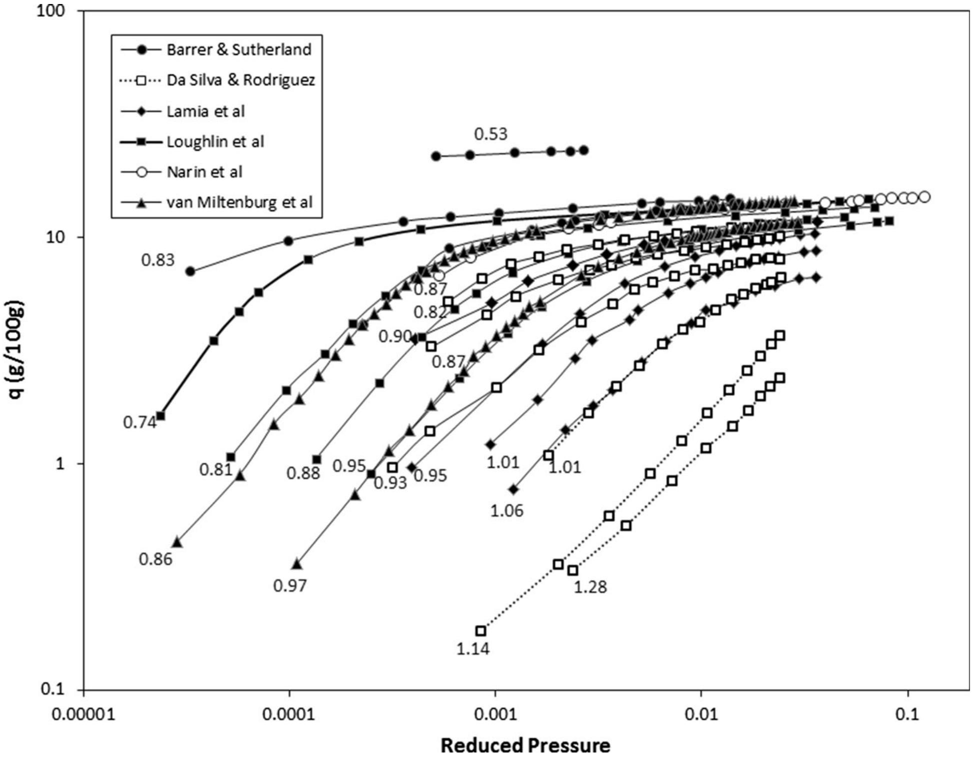

0.70 to 0.81. The n-butane isotherms show excellent agreement in the entire pressure range covered and hence neither modification nor any point deletion is required. This is expected since only a single study is available from Barrer and Sutherland (1956). The isotherms are shown in a log–log plot in Figure S5b. It should be noted that all these isotherms tend to be in the saturation region, so that no data exists for the Henry Law region.

The iso butane data are from four different studies, Hyun and Danner (1982), Lamia et al. (2007), Campo et al. (2014) and Barrer and Sutherland (1956). Figure S6a shows the isotherms for branched butane ranging from a T_r of 0.73 to 1.04. The iso butane isotherms from Campo et al. (2014) appears to be inconsistent in shape and position and so are deleted. Isotherms from the other three studies in general are consistent in shape and position with some exceptions. Data from Hyun and Danner (1982) and Lamia et al. (2007) are similar in both low and high pressure ranges, but the Barrer and Sutherland (1956) isotherms are slightly higher. Iso butane data at a T_r of 0.79 from Hyun and Danner is lying between isotherms at a T_r of 0.87 and 0.82 from Lamia et al. (2007) which suggest a slight position inconsistency. However, the isotherms from all three studies are close to each other and hence all are retained. As may be observed from Figure S6a, iso butane isotherms from Hyun and Danner (1982) and Lamia et al. (2007) are leveling off a bit earlier than those from Barrer and Sutherland (1956).

As per the criteria for choosing the saturation loading from the experimental data, Figs. 5 and S6b suggest that all branched butane isotherms are saturated. Barrer and Sutherland's isotherms do not exhibit any low concentration data. The isotherms of Lamia et al. and Hyun and Danner do. The three isotherms with the highest T_r on the right of the plot exhibit slopes of 1 at low loading although one of the isotherms appears to have a slight sigmoidal shape. The three isotherms on the left of the plot do not extend sufficiently into low concentration data to be in the Henry Law region.

Normal, iso and neo pentane isotherms are found in a single study by Barrer and Sutherland (1956). Each is reviewed separately.

In Figure S7a, n pentane isotherms show excellent agreement in the entire pressure range which is expected since they are sourced from the same study as mentioned earlier. Similarly, iso pentane and neo pentane isotherms show excellent agreement in the entire pressure range as can be seen from Figures S8a and S9a respectively. Hence, neither modification nor isotherm deletion is required.

The straight pentane isotherms are plotted on a log–log plot in Figure S7b. As per the criteria for choosing the saturation loading from the experimental data, straight pentane from a T_r of 0.64 to 0.73 all appear to be levelling off and all are included for saturation calculations. None of these isotherms extend into the low concentration Henry Law region.

Iso pentane isotherms ranging from a T_r of 0.65 to 0.75 are plotted in the standard form in Figure S8a and on a log–log plot in Figure S8b. The iso pentane isotherms all appear to be approaching saturation as they are all levelling off. They are all included in the saturation q_{max} calculation. None of these isotherms extend into the low concentration Henry Law region.

Neo pentane isotherms from a T_r of 0.69 to 0.79 are plotted in the standard form in Figure S9a and on a log–log plot in Figure S9b. The neo pentane isotherms all appear to

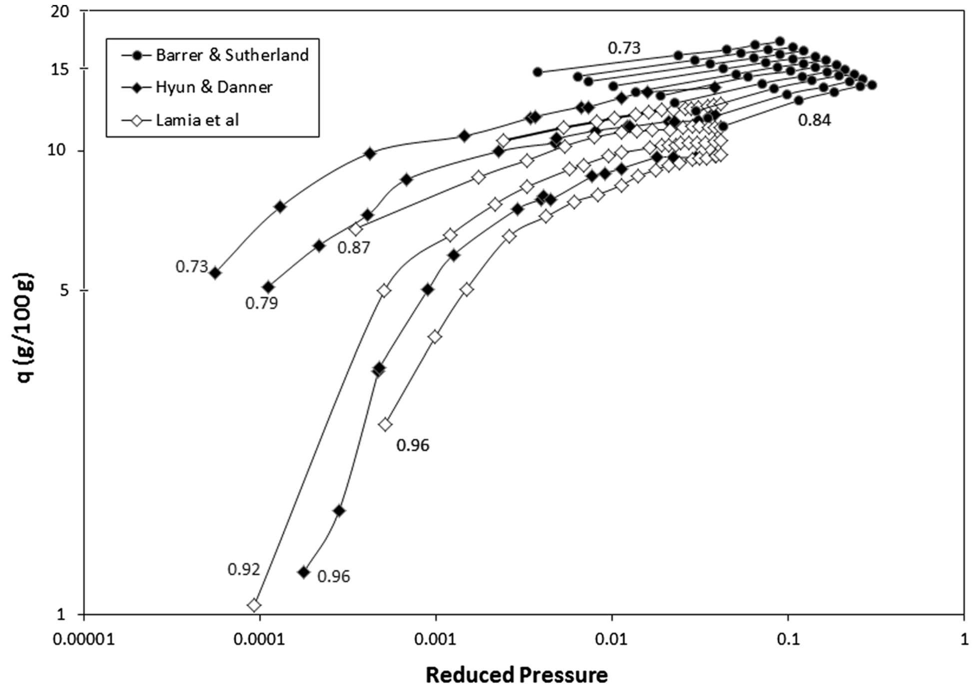

Fig. 5 Log–log plot of iso butane isotherms. Labels are reduced temperatures. Isotherms that attain saturation have a *solid line*

be approaching saturation as they are all levelling off. They are all included in the saturation q_{max} calculation. None of these isotherms extend into the low concentration Henry Law region. Further, the saturation values for the neo pentane isotherms range between 12.5 and 14.0 g/100 g, which are lower than those observed for the normal or iso pentane at between 16.4 and 18.8 g/100 g. This is probably a reflection of a steric effect for packing in neo pentane molecules into the zeolite cavity.

Normal hexane isotherms are plotted in Figures S10a and S10b. These are collected from two different studies, Barrer and Sutherland (1956) and Zhdanov et al. (1962). They range from a T_r of 0.59 to 0.68, and include two isotherms from Zhdanov et al. (1962), both at a T_r of 0.59, one on a porous 13X crystal and the other on a pelleted sample of Linde 13X. Note that both isotherms are presented on a crystal basis. It is observed that the isotherm measured on the pelleted sample (the lowest isotherm) is lower than the isotherm from the crystal sample, and also lower than the Barrer and Sutherland (1956) isotherms. This isotherm is deleted (shown in grey). The isotherm on the pelleted sample also exhibited capillary condensation since the binder promotes this phenomenon while the isotherm measured on porous crystal does not.

The hexane isotherms are plotted in Figure S10b after screening. As per the criteria for choosing the saturation loading from the experimental data, all hexane isotherms are considered for further study as they leveled off to the saturation limit as may be observed from the Figure. Further, there is no Henry Law data as low concentration ranges are omitted.

Heptane isotherms collected from two different studies by Barrer and Sutherland (1956) and Ruthven and Doetsch (1976) are plotted in Figure S11a; they range from a T_r of 0.55 to 0.90. As may be observed all isotherms appear to be consistent in shape and position and hence neither deletion nor modification is required. It is clear that the studies are from two different concentration regions; the study of Barrer and Sutherland is limited to the high concentration region whereas that of Ruthven and Doetsch extends over the entire range. Further, the three lower isotherms for Ruthven and Doetsch appear to exhibit capillary condensation at their highest point. These points have been deleted (grey points).

The isotherms are plotted on a log–log scale in Figs. 6 and S11b. As per the criteria for choosing the saturation loading from the experimental data, all heptane isotherms have plateaued to the saturation limit and hence all are included in the saturation q_{max} observations. The isotherms of Barrer and Sutherland have no Henry Law component; the three lowest isotherms of Ruthven et al. appear to have a slope of 1 at low loading and are in the Henry Law region. Their top isotherm at T_r of 0.76 has insufficient low concentration data.

Normal and iso octane isotherms are found in a single study by Barrer and Sutherland (1956). The n octane isotherms before screening are plotted in Figure S12a. They range from a T_r of 0.55 to 0.60. The straight octane

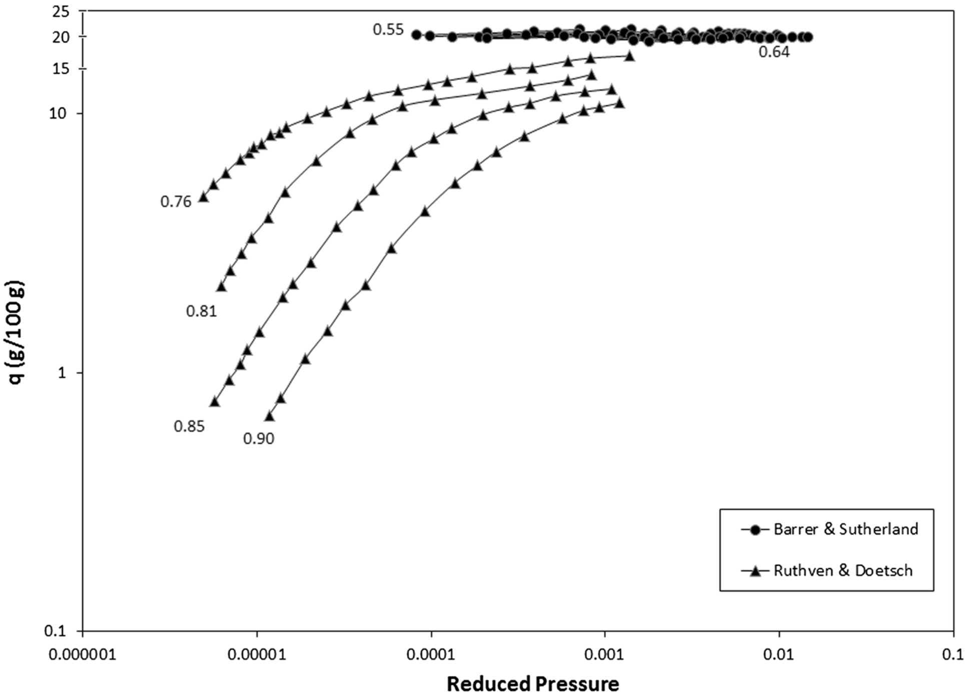

Fig. 6 Log–log plot of n-heptane isotherms. Labels are reduced temperatures. Isotherms that attain saturation have a *solid line*

isotherms in Figure S12a show excellent agreement in the entire pressure range which is expected since they are sourced from the same study. Two isotherms have been modified. The top 3 points of the n-octane isotherm at a T_r of 0.55 and at a T_r of 0.59 are omitted as they represent capillary condensation (grey points). The isotherms are plotted in a log–log plot in Figure S12b. As per the criteria for choosing the saturation loading from the experimental data, all the straight octane isotherms after these corrections are considered saturated and hence included in the q_{max} calculation. There is no Henry Law data.

Iso octane isotherms are plotted in Figure S13a for the range T_r 0.55–0.63. All the isotherms are consistent over the entire pressure range as is to be expected for a single study. The top four isotherms exhibit capillary condensation and are modified. The data points shown in grey are considered capillary condensation and are deleted.

All the remaining points are plotted on a log–log plot in Figure S13b. The data are consistent, approaching a limit and are all included in the q_{max} calculation. The data contain no Henry law data.

The maximum saturation concentrations for all the species are plotted in Figs. 7 and S14 as q_{max} versus T_r. The plot is separated into two regions, a subcritical region to the left of $T_r = 1$ and a supercritical region to the right of $T_r = 1$. The data in the subcritical region lie between the predicted saturation loadings for C_1 and C_8, indicated by the solid lines in the Figure. Some data points are outside the upper C_8 line; these will be shown in Figs. 8a and S15b to be due to one particular study. The data in the subcritical region for any particular species demonstrate the same shape as illustrated in Fig. 1 for the theoretical calculation for q_{max}.

The data in the supercritical region lie between two bounding lines at $q_{max} = 6$ and 11 g/100 g. The data above a T_r of 1.1 are all for methane. Data for ethane and propane, just slightly above $T_r = 1$ are also within the bounding lines. There is no consistent pattern to the experimental data in this region; hence the use of a fixed range of

$$q_{max} = 8.5 \pm 2.5 g/100g, \tag{7}$$

may be appropriate for the supercritical region. This is similar to the observation made for supercritical alkanes on 5A zeolite (Loughlin and Abouelnasr 2009); the range for 5A was reported as 7–9 g/100 g, or 8 ± 1 g/100 g.

The observed data are also plotted as a normalized parameter Γ, calculated using Eq. 7, versus T_r in Figs. 8b and S15a. The model is represented as a solid line in the Figure, and is defined by Eq. 6. In our previous paper, Loughlin and Abouelnasr (2009), we demonstrated that critical adsorbate reduced temperature is lower than the critical temperature for the VLE data. This suggests using a lower T_C for the adsorbate may be appropriate but we lack data to justify it for 13X.

Again in Fig. 8a, a subcritical region and a supercritical region may be observed. All the data in the subcritical region lies adjacent to the theoretical normalized gamma plot. Note that the neo pentane data are well below the theoretical model. This will be discussed in more detail later. Some of the data are above and some below the curve. However, there should be none above the

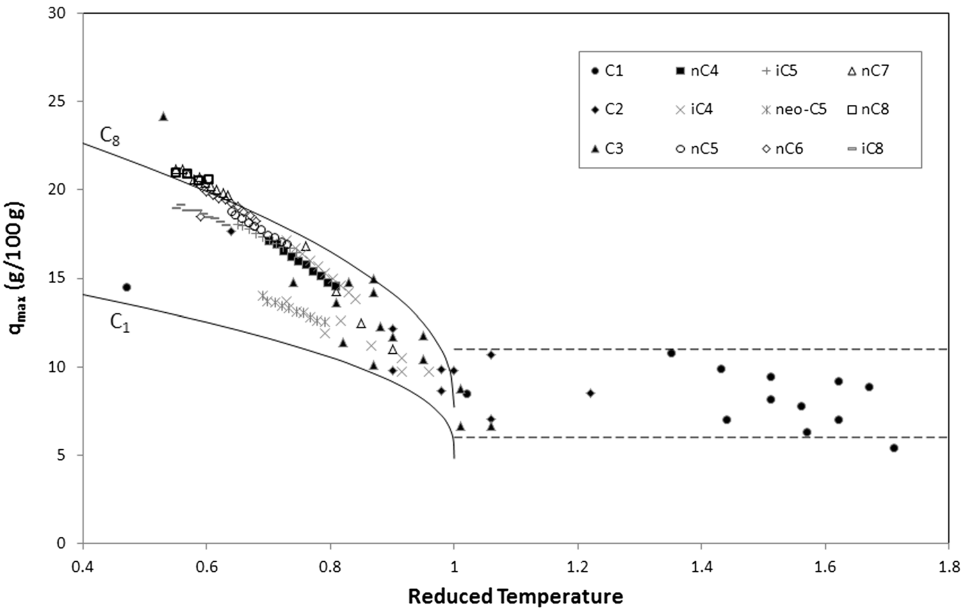

Fig. 7 q_{max} versus T_r for all alkanes. *Bounding-lines* for supercritical are at 6 and 11 g/100 g

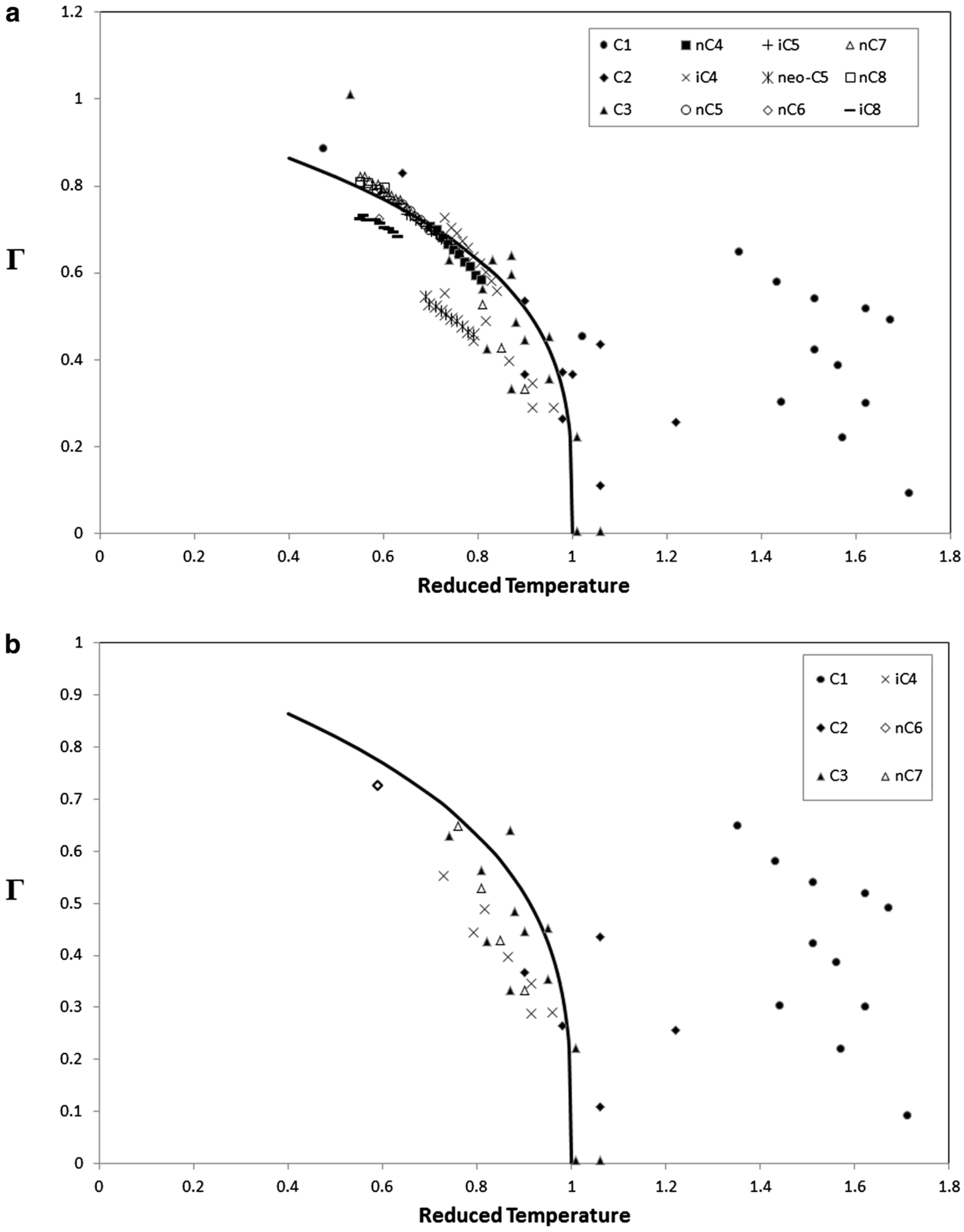

Fig. 8 **a** *Solid line* is the theoretical plot of normalized parameter Γ against reduced temperature, Eq. 6. Points are Γ derived from the observed values for q_{max}, per Eq. 7. **b** Same as Fig. 8a, but with Barrer and Sutherland data removed. **c** *Solid line* is the theoretical plot of normalized parameter Γ against reduced temperature, Eq. 6. Points are Γ derived from the observed values for q_{max}, per Eq. 7, for only branched alkanes. **d** *Solid line* is the theoretical plot of normalized parameter Γ against reduced temperature, Eq. 6. Points are Γ derived from the observed values for q_{max}, corrected by the steric factor per Eq. 7, for only branched alkanes

theoretical plot as that implies Eq. 3 is exceeded which is theoretically infeasible. To establish the reason for this discrepancy, the data are replotted without individual studies. It is observed that when all the Barrer and Sutherland (1956) data is removed, the plot illustrated in Fig. 8b is obtained. It is clear that almost all the data is now on or below the theoretical line. This suggests that, in Barrer and Sutherland's data which they plotted on a hydrated basis, the original sample may not have contained as much moisture as reported in their paper (25.3 % by weight). The data in the supercritical region exhibits no pattern; more data is required to establish a pattern.

As observed in Fig. 8a, the data for neo pentane are well below the model. This is illustrated in more detail in Figs. 9 and S16. The theoretical model and observed data are plotted for n–, iso–, and neo pentane. Data for all three isomers came from Barrer and Sutherland (1956). Both the n- and the iso-pentane are in good agreement with their respective models. But neo pentane is far below its model. This is likely due to steric effects. A steric factor λ must be introduced into Eq. 3 giving

$$q_{\max}\left(\frac{g}{100gZ}\right) = \lambda 100\frac{\varepsilon_Z}{\rho_Z}\left(\frac{P_c MW}{RT_c}\right)Z_{RA}^{-\left\{1+(1-T_r)^{0.2857}\right\}}. \tag{8}$$

Fig. 8 continued

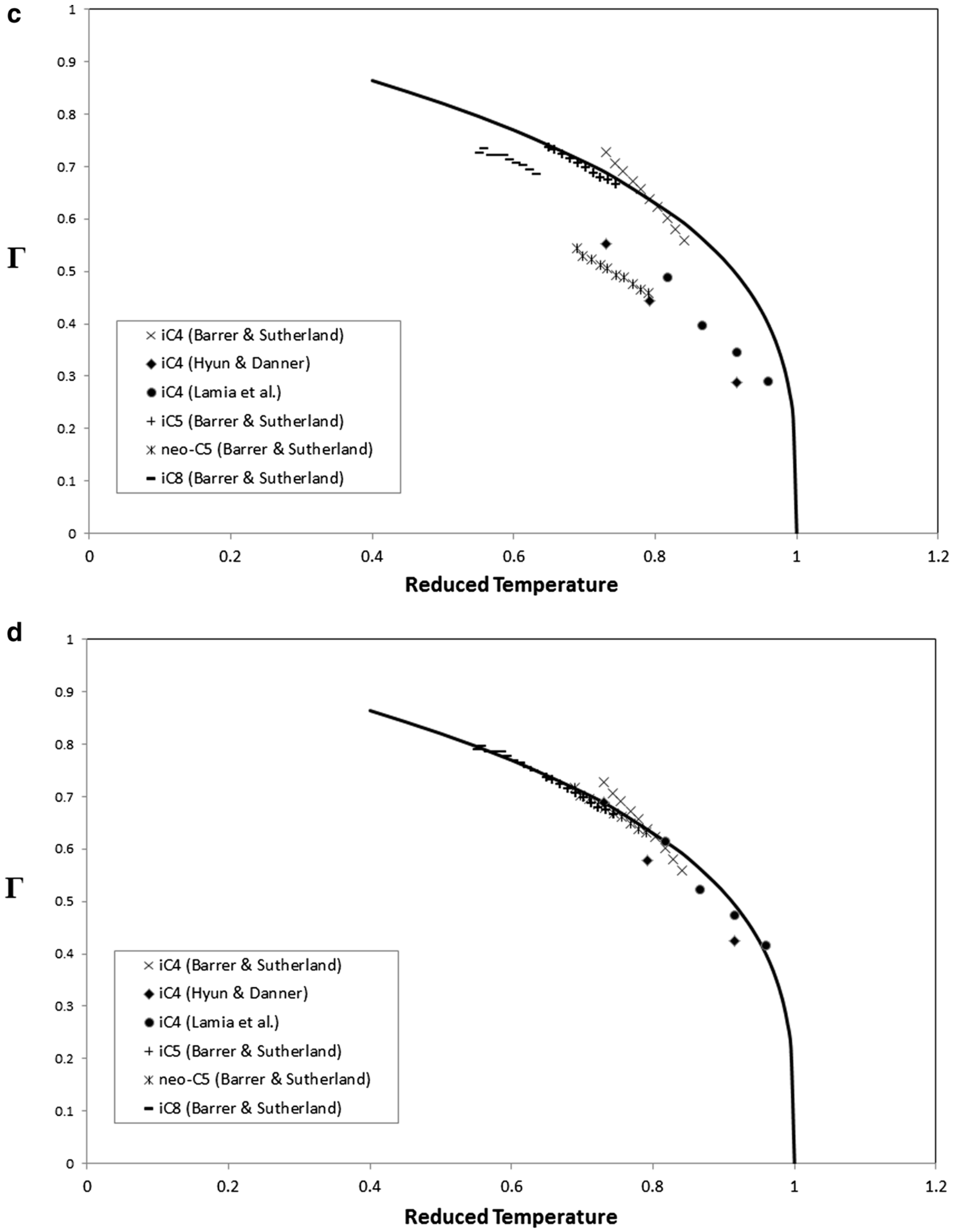

The theoretical model incorporating the steric factors and observed values for q_{max} are plotted in Fig. 9 for the pentane data from Barrer and Sutherland's study, showing the excellent fit. The fit for neo pentane with a steric factor of 0.80 suggests that only 80 % of the zeolite cage is filled by neo pentane on saturation. However, as the data for neo pentane are from Barrer and Sutherland (1956), then the data could be too high. In this case, the steric effects could be even greater.

A reviewer of this paper pointed out that we should also consider steric factors for all the other iso alkane samples as they also did not appear to be consistent with the model. To illustrate the problem, the iso and neo alkanes are plotted separately in Figs. 8c and S15c and it is clear that data from studies other than Barrer and Sutherland, are also below the theoretical model. Steric factors are calculated using Eq. 8 and tabulated in Table 2 separated by study. Iso butane data from Hyun and Danner and from Lamia et al. both require a steric factor of around 0.85. Although the iso alkane data of Barrer and Sutherland is in good agreement with the model, this may be due to an incorrect percentage dehydration in their original sample. With the incorporation of these steric factors, the fit of the model with the data is excellent as shown in Figs. 8d and S15d.

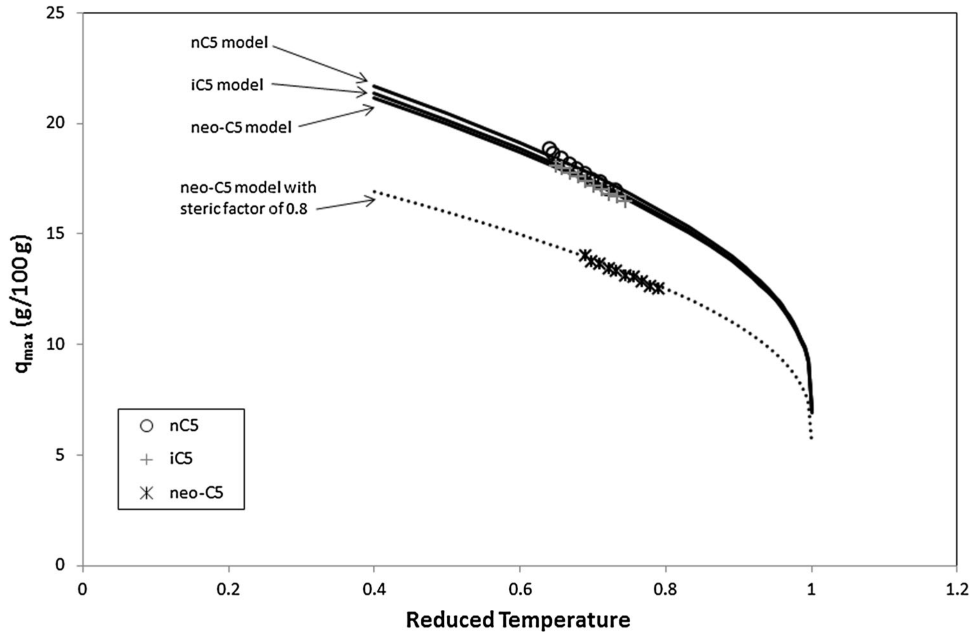

Fig. 9 The model and observed q_{max} for all three isomers of pentane. The model for neo pentane with a steric factor of 0.8 is indicated by a *dotted line*

Table 2 Steric factors for iso alkanes and neo pentane

Alkane	Barrer and Sutherland	Hyun and Danner	Lamia et al.
Iso butane	1	0.84	0.85
Iso pentane	1		
Iso octane	0.92		
Neo pentane	0.80		

5 Conclusions

The published experimental adsorption isotherms of n-, iso- and neo alkanes, C_1 to C_8 in 13X zeolite are evaluated for consistency using semi-log plots of the isotherms for each species. Several studies are found to be relatively consistent for six of the species. Several other species are reported by only a single study, Barrer and Sutherland (1956). The isotherms are then evaluated to determine whether they attained or approached saturation using log–log plots of the isotherms. The maximum experimental adsorption of those isotherms at or near saturation is recorded.

The experimental data fall into two regions, a subcritical region and a supercritical region. In the subcritical region, a model is proposed for saturation loading using the modified Rackett equation of Spencer and Danner (1972) for saturated liquid densities combined with crystallographic data for the 13X zeolite. The maximum experimental adsorption for n- and most iso-alkanes validate the proposed model. Steric factors are required for neo pentane and some iso alkanes depending on the study. In the supercritical region the saturation loading is ill-defined. A correlation equation of $q_{max} = 8.5 \pm 2.5$ g/100 g satisfactorily fits the data. The use of the upper bound of 11 or 12 g/100 g is recommended in the absence of sufficient data.

Acknowledgments This is a detailed manuscript of a paper presented at the Fall 2011 conference of AICHE. The authors wish to acknowledge the support of the American University of Sharjah and the California State University at Bakersfield during this study. The authors also wish to acknowledge anonymous reviewers for their comments on steric factors.

References

Al Mousa, A., Abouelnasr, M., Loughlin, K.: Saturated loadings on 13X (faujasite) zeolite above and below the critical conditions. Part II: unsaturated and cyclic hydrocarbons data evaluation and modeling, Adsorption (2015a). doi:10.1007/s10450-015-9671-y

Al Mousa, A., Abouelnasr, M., Loughlin, K.: Saturation loadings on 13X (faujasite) zeolite above and below the critical conditions. Part III: inorganic, and ethyl acetate data evaluation and modeling, unpublished work, (2015b)

Barrer, R., Sutherland, J.W.: Inclusion complexes of faujasite with paraffins and permanent gases. Proc. R. Soc. Lond. A **237**(1211), 439–463 (1956)

Breck, D.: Zeolite Molecular Sieves; Structure, Chemistry and Use. Wiley, New York (1974)

Campo, M., Baptista, M., Ribeiro, A., Ferreira, A., Santos, J., Lutz, C., Rodrigues, A.: Gas phase SMB for propane/propylene separation using enhanced 13X zeolite beads. Adsorption **20**, 61–75 (2014)

Campo, M., Ribeiro, A., Ferreira, A., Santos, J., Lutz, C., Loueiro, J.A.: New 13X zeolite for propylene/propane separation by vacuum swing adsorption. Sep. Purif. Technol. **103**, 60–70 (2013)

Cavenati, S., Grande, C., Rodrigues, A.: Adsorption equilibrium of methane, carbon dioxide, and nitrogen on zeolite 13X at high pressures. J. Chem. Eng. Data **49**(4), 1095–1101 (2004)

CHERIC. http:www.cheric.org/kdb/research/hcprop/cmpsrch.phpe. Accessed 27 Mar 2012

Da Silva, F., Rodrigues, A.: Adsorption equilibria and kinetics for propylene and propane over 13X and 4A zeolite pellets. Ind. Eng. Chem. Res. **38**(5), 2051–2057 (1999)

Hyun, S., Danner, R.P.: Equilibrium adsorption of ethane, ethylene, isobutane, carbon dioxide, and their binary mixtures on 13X molecular sieves. J. Chem. Eng. Data **27**(2), 196–200 (1982)

Lamia, N., Wolff, L., Leflaive, P., Sa Gomes, P.: Propane/propylene separation by simulated moving bed I. Adsorption of propane, propylene and isobutane in pellets of 13X zeolite. Sep. Sci. Technol. **42**(12), 2539–2566 (2007)

Lopes, F.V., Grande, C.A., Ribeiro, A.M., Loureiro, J.M., Evaggelos, O., Nikolakis, V., Rodrigues, A.E.: Adsorption of H_2, CO_2, CH_4, CO, N_2 and H_2O in activated carbon and zeolite for hydrogen production. Sep. Sci. Technol. **44**(5), 1045–1073 (2009)

Loughlin, K.F., Abouelnasr, D.M.: Sorbate densities on 5A zeolite above and below the critical conditions: n alkane data evaluation and modeing. Adsorption **15**, 521–533 (2009)

Loughlin, K., Hasanain, M., Abdul-Rehman, H.: Quaternary, ternary, binary, and pure component sorption on zeolites. 2. light alkanes on Linde 5A and 13X zeolites at moderate to high pressures. Ind. Eng. Chem. Res. **29**(7), 1535–1546 (1990)

Narin, G., Martins, V.F., Campo, M.R.A., Ferreira, A., Santos, J.C., Rodrigues, A.E.: Light olefins/paraffins separation with 13X zeolite binderless beads. Sep. Purif. Technol. **133**, 452–475 (2014)

Rolniak, P.D., Kobayashi, R.: Adsorption of methane and several mixtures of methane and carbon dioxide at elevated pressures and near ambient temperatures on 5A and 13X molecular sieves by tracer perturbation chromatography. AIChE J. **26**(4), 616–625 (1980)

Ruthven, D., Doetsch, I.: Diffusion of hydrocarbons in 13X zeolite. AIChE J. **22**(5), 882–886 (1976)

Salem, M.M., Braeuer, P., Szombathely, M.V., Heuchel, M., Harting, P., Quitzsch, K.: Thermodynamics of high-pressure adsorption of argon, nitrogen, and methane on microporous adsorbents. Langmuir **14**(12), 3376–3389 (1998)

Spencer, C., Danner, R.: Improved equation for prediction of saturated liquid density. J. Chem. Eng. Data **17**(2), 236–240 (1972)

van Miltenburg, A., Gascon, J., Zhu, W., Kapteijn, F., Moulijn, J.A.: Propylene/propane mixture adsorption on faujasite sorbents. Adsorption **14**(2–3), 309–321 (2008)

Vermesse, J., Vidal, D., Malbrunot, P.: Gas adsorption on zeolites at high pressure. Langmuir **12**(17), 4190–4196 (1996)

Zhdanov, S.P., Kiselev, A.V., Pavlova, L.F.: Adsorption of benzene and n-hexane and their liquid solutions by 10X and 13X zeolites. Kinet. Katal. **3**(3), 391–394 (1962)